

**CRYSTAL ENGINEERING OF GROUP(II) AND Mn(II)  
BASED COORDINATION POLYMERS (CPs) WITH  
SELECTED DICARBOXYLATES AND THEIR  
DIELECTRIC PROPERTIES**

**BALENDRA**



**DEPARTMENT OF CHEMISTRY  
INDIAN INSTITUTE OF TECHNOLOGY DELHI  
DECEMBER 2018**

©Indian Institute of Technology Delhi (IITD), New Delhi, 2018

**CRYSTAL ENGINEERING OF GROUP(II) AND Mn(II)  
BASED COORDINATION POLYMERS (CPs) WITH  
SELECTED DICARBOXYLATES AND THEIR  
DIELECTRIC PROPERTIES**

*by*

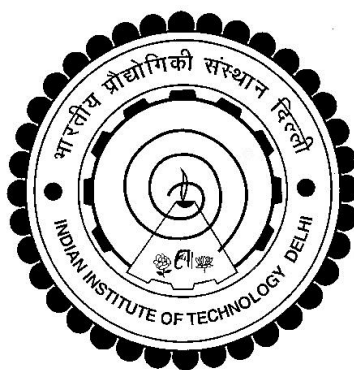
**BALENDRA**

**DEPARTMENT OF CHEMISTRY**

*Submitted*

*In fulfillment of the requirements of the degree of Doctor of Philosophy*

*to the*



**INDIAN INSTITUTE OF TECHNOLOGY DELHI**

**DECEMBER 2018**

*Dedicated*  
*To*  
*my brother and father*

## CERTIFICATE

This is to certify that the thesis entitled, “**Crystal engineering of Group(II) and Mn(II) based coordination polymers (CPs) with selected dicarboxylates and their dielectric properties**” being submitted by **Mr. Balendra** to the Indian Institute of Technology Delhi for the award of the degree of **Doctor of Philosophy** in Chemistry, is a record of bonafide research work carried out by him. Mr. Balendra has worked under my guidance and supervision and has fulfilled the requirements for the submission of this thesis, which to my knowledge has reached the requisite standard.

The results contained in this dissertation have not been submitted, in part or full, to any other university or institute for award of any degree or diploma.

**Dr. A. RAMANAN**  
Professor  
Department of Chemistry  
Indian Institute of Technology Delhi  
New Delhi-110016

## ACKNOWLEDGEMENTS

I express my sincere gratitude to my supervisor **Prof. A. Ramanan** for his guidance and valuable suggestions. Without his co-operation and support this thesis would not have taken the following shape.

I wish to express my sincere thanks to the heads of the Department of Chemistry, Prof. A. Ramanan and Prof. A. K. Singh for their valuable contribution and support throughout my Ph.D work at IIT Delhi. I would also like to thank all the staff associated with the Department of Chemistry, IIT Delhi. My sincere thank goes to Prof. S. Murugavel and Azeem Banday, Department of Physics & astrophysics University of Delhi, for dielectric properties characterization and valuable discussion on the dielectric behavior. I am highly obliged to Dr. G. Vijaya Prakash and Dr. Pawan K. Kanaujia, Nanophotonics Lab, Department of Physics, Indian Institute of Technology Delhi, for optical properties characterization. The discussion with them enabled me to understand the optical properties. I would like to thank my college chemistry teachers Dr. Sangeeta Pandita, Dr. Vijay Sharda, Dr. Shulekh Chandra for helping me throughout my graduation periods and inspiring me to pursue my career in research.

My special thanks to my MSc classmates (Amit, Surjo, Abhishek, Tushar, Sami, Sourav, Venky, Monalisa, Deepa, Sapna, Soumita, Bratati and Sunita) of Indian Institute of Technology Roorkee. Our association goes a very long since day of post-graduation and they have been with me ever since then as a friend. Special thanks to my best buddies, Sourav, Sami and Tushar for being with me in thicks and thins of life, I find myself lucky to have friends like them in my life.

I express my sincere thanks to my seniors Dr. Minakshi Asnani, Dr. Pavani, Dr. Purnendu Parhi, Dr. Shailesh Upreti, Dr. Jency Thomas, Dr. Kalawati Saini, Dr. Monika Singh and Dr. Dinesh Kumar. I thank my colleagues Dr. Pramod Kumar, Dr. Vineet Kumar, Dr. Manju, Shailabh, Maneesha and Bharti for creating wonderful friendly atmosphere in the lab. I also thank to, Babita Shakya, Anuradha, Amit and Azad. I would also like to thank my friends Soumen, Zeba, Sourab, Mahendra, Abhijit, Pawan and Rajendra Singhla for making my stay comfortable. Words are no measure to describe the forbearance and fortitude with which my wife Mrs. Sanyukta encouraged me. I thank her for being so understanding and for putting up with me through the toughest moments of my life. It is because of the great support and encouragement of my wife, which enabled me to successfully complete my work. The unconditional love and blessings of my late father and mother made me what I am today and I owe everything to them. I express my intense feeling and gratitude towards my brothers, sisters, brother-in laws and sister-in-laws. Sweet thank is also for my nephew Aarav (Sawan) and neice Khushi for their puerile support.

Lastly, and most importantly, I wish to thank my elder brother, Jugmendra Singh (Assistant Professor, Department of Chemistry, DeshBandhu College Delhi University). My life would be nowhere without him. He helped me to shape my career at every point of my life and always supported me financially, morally and spiritually. I don't know how to thank him for providing me with the opportunities to be where I am today. I am really lucky to have him as a brother in my life. I dedicate my Ph.D thesis to him.

Balendra

## Abstract

Crystal engineering focuses on the intentional design of functional solids with desired physical and chemical properties. Crystal engineers commonly use supramolecular synthon approach to simplify the difficult task of analyzing complex supramolecular architectures as well as to construct the desired supermolecule. The supramolecular synthon concept can be extended to discrete coordination complex based solids as well as extended ones like coordination polymers (CPs) and metal-organic frameworks (MOFs). Crystallization of new solids like CPs or MOFs with multidimensional networks is currently being explored with an objective to isolate structures with predictable frameworks and ability to incorporate functional properties. The conventional synthetic strategies for the construction of CPs/MOFs involve coordination of one type of linker with a single metal. The other synthetic strategy involves the addition of an auxiliary ligand, mostly a N-donor based along with a multidentate linker which offer more structural diversity and functionality. CPs/MOFs have been sought as potential materials for gas storage and separation but less attention has been made to employ them in microelectronic devices. Recently, a few CPs/MOFs based on group(II) metals showed promising dielectric behavior such as low- $\kappa$  materials owing to rigid metal-carboxylate interaction which provides less flexibility to the framework. Unlike, transition metals, group(II) metal based carboxylates have been less explored. In this work, we plan to investigate supramolecular assemblies built of the reliable and chemically reasonable building blocks. For this purpose, we opted two strategies: At first, we conducted several crystallization reactions between different metals of group(II) and one dicarboxylate ligand to explore the structural landscape of alkaline-earth-carboxylate system. In the second strategy, we examined the role of a single metal with different dicarboxylates to obtain novel

structures that are built through H-bonding (0D) and metal-carboxylate interaction (1D, 2D and 3D). We intended to isolate new solids that exhibit interesting optical and dielectric properties and hence we preferred alkaline-earth or Mn(II) metal. In contrast to transition metals, alkaline-earth metals showed a higher coordination number with more flexible geometry; this makes crystal engineering more interesting but also difficult to predict.

Chapter I provides a brief account of our literature survey on the crystal engineering of alkaline-earth and Mn(II) based CPs/MOFs as well as motivation for the present work. Chapter II explored the structural landscape of the system containing divalent alkaline-earth metal ions (Mg, Ca and Sr) with 2,5-thiophenedicarboxylic acid (*TDC*) under varying solvothermal condition in different aprotic solvents (DMF, DMA and DEF). Crystal structures of resulted solids were characteristic of extended coordination interaction between metal and carboxylate ions resulting in column based structures. All the solids showed a blue emission arising from intra ligand charge transfer.

Chapter III is divided into two parts. In chapter IIIA we explored the synthesis-structure correlation where we systematically investigated the structural landscape of calcium and strontium based dicarboxylates under solvothermal condition. Two rigid and two flexible organic ligands were used in three aprotic polar solvents *viz.* DMF, DMA, and MF. A significant structural feature of all the solids was the occurrence of rigid 1D columns made of metal-carboxylate coordination. As to intrinsic properties, all the six solids showed interesting dielectric behaviour at different temperatures and frequencies. All the solids exhibited photoluminescence with blue or bluish-green emission. In chapter IIIB, we have explored the solvothermal crystallization of strontium ions with three different carboxylic acids containing pyridine or amino group with an objective to rationalize the supramolecular

organization of strontium ions with carboxylate groups. Use of multidentate linkers (2,5-*PDC*) and (2-*PZC*) led to 3D CPs driven by 1D strontium carboxylate columns linked by organic bridges. A flexible aminodicarboxylic acid such as *IDA* led to another interesting solid wherein a rather rare discrete  $\text{SrO}_6$  is linked to each other through the organic linker forming a sheet. Frequency and temperature dependent dielectric behavior of four newly prepared solids were investigated. In chapter IV, two V-shaped ligands were chosen to prepare the different coordination polymers. Literature showed that, most of the MOFs/CPs formed by these two V-shaped ligands have enough space to accommodate guest molecules in the structure. So, our primary motive was to prepare alkaline-earth metals based MOFs/CPs with or without guest molecules and investigate guest dependent dielectric behavior of the solids. In chapter V, we extended our work with 4,4-sulfonyldibenzoic acid and prepared a variety of coordination polymers with manganese salts and N-containing auxiliary ligands. Auxiliary ligands, in particular N-donor based ones along with a dicarboxylate ligand offered more structural diversity. In this chapter, we report crystallization of nine new CPs based on Mn(II) along with dielectric measurement and magnetic properties. Chapter VI summarises the various results obtained in this study and conclusions drawn from it. We also have suggested a few possible directions for future work.

## सार

क्रिस्टल इंजीनियरिंग वांछित भौतिक और रासायनिक गुणों के साथ कार्यात्मक ठोस के जानबूझकर डिजाइन पर केंद्रित है। क्रिस्टल इंजीनियरों आमतौर पर जटिल सुपरमोल्यूलर आर्किटेक्चर का विश्लेषण करने के साथ-साथ वांछित सुपरमोल्यूलर का निर्माण करने के कठिन कार्य को सरल बनाने के लिए सुपरमोल्यूलर सिंथॉन दृष्टिकोण का उपयोग करते हैं। सुपरमोल्यूलर सिंथॉन अवधारणा को पृथक समन्वय परिसर आधारित ठोस के साथ-साथ समन्वय पॉलिमर (सीपी) और धातु-जैविक ढांचे (एमओएफ) जैसे विस्तारित लोगों तक बढ़ाया जा सकता है। बहु-आयामी नेटवर्क वाले सीपी या एमओएफ जैसे नए ठोस पदार्थों का क्रिस्टलाइजेशन वर्तमान में पूर्वानुमानित ढांचे और कार्यात्मक गुणों को शामिल करने की क्षमता के साथ संरचनाओं को अलग करने के उद्देश्य से खोजा जा रहा है। सीपी / एमओएफ के निर्माण के लिए पारंपरिक सिंथेटिक रणनीतियों में एक धातु के साथ एक प्रकार के लिंकर का समन्वय शामिल है। अन्य सिंथेटिक रणनीति में एक सहायक लिगैंड के अतिरिक्त शामिल हैं, अधिकांशतः एन-दाता एक बहुआयामी लिंकर के साथ-साथ अधिक संरचनात्मक विविधता और कार्यक्षमता प्रदान करता है। सीपी / एमओएफ को गैस भंडारण और अलगाव के लिए संभावित सामग्रियों के रूप में मांगा गया है लेकिन माइक्रोइलेक्ट्रॉनिक उपकरणों में उन्हें नियोजित करने के लिए कम ध्यान दिया गया है। हाल ही में, समूह (द्वितीय) धातुओं के आधार पर कुछ सीपी / एमओएफ ने कठोर धातु-कार्बोक्साइलेट इंटरैक्शन के कारण कम- $k$  सामग्री जैसे ढांकता हुआ व्यवहार दिखाया जो ढांचे को कम लचीलापन प्रदान करता है। विपरीत, संक्रमण धातुओं, समूह (द्वितीय) धातु आधारित कार्बोक्साइलेट्स की खोज कम हो गई है। इस काम में, हम भरोसेमंद और रासायनिक रूप से उचित बिल्डिंग ब्लॉक के बने सुपरमोल्यूलर असंबली की जांच करने की योजना बना रहे हैं। इस उद्देश्य के लिए, हमने दो रणनीतियों का चयन किया: सबसे पहले, हमने क्षारीय-पृथ्वी-कार्बोक्साइल प्रणाली के संरचनात्मक परिदृश्य का पता लगाने के लिए समूह (द्वितीय) और एक डाइकरबॉक्साइलेट लिगैंड के विभिन्न धातुओं के बीच कई क्रिस्टलाइजेशन प्रतिक्रियाएं आयोजित कीं। दूसरी रणनीति में, हमने एच-बॉन्डिंग (0 डी) और धातु-कार्बोक्साइलेट इंटरैक्शन (1 डी, 2 डी और 3 डी) के माध्यम से बनाए गए उपन्यास संरचनाओं को प्राप्त करने के लिए विभिन्न डिकारोक्साइलेट्स के साथ एक एकल धातु की भूमिका की जांच की। हम नए ठोस पदार्थों को अलग करना चाहते थे जो दिलचस्प ऑप्टिकल और ढांकता हुआ गुण प्रदर्शित करते थे और इसलिए हमने क्षारीय-पृथ्वी या एमएन (द्वितीय) धातु को प्राथमिकता दी। संक्रमण धातुओं के विपरीत, क्षारीय-पृथ्वी धातुओं ने अधिक लचीली ज्यामिति के

साथ एक उच्च समन्वय संख्या दिखायी; यह क्रिस्टल इंजीनियरिंग को और अधिक रोचक बनाता है लेकिन भविष्यवाणी करना भी मुश्किल है।

अध्याय में क्षारीय-पृथ्वी और एमएन (द्वितीय) आधारित सीपी / एमओएफ के क्रिस्टल इंजीनियरिंग के साथ-साथ वर्तमान कार्य के लिए प्रेरणा पर हमारे साहित्य सर्वेक्षण का एक संक्षिप्त विवरण प्रदान करता हूं। अध्याय II ने विभिन्न सॉल्वेंट्स (डीएमएफ, डीएमए और डीईएफ) में अलग-अलग स्थिति के तहत एसिड (टीडीसी) के साथ क्षारीय-पृथ्वी धातु आयनों (एमजी, सीए और सीनियर) युक्त प्रणाली के संरचनात्मक परिदृश्य की खोज की। परिणामी ठोस पदार्थों की क्रिस्टल संरचनाएं धातु और कार्बोक्साइल आयनों के बीच विस्तारित समन्वय बातचीत की विशेषता थी जिसके परिणामस्वरूप कॉलम आधारित संरचनाएं थीं। सभी ठोस पदार्थों ने इंट्रा लिगेंड चार्ज ट्रांसफर से उत्पन्न नीले उत्सर्जन को दिखाया।

अध्याय III दो भागों में बांटा गया है। अध्याय IIIA में हमने संश्लेषण-संरचना सहसंबंध की खोज की जहां हमने व्यवस्थित रूप से कैल्शियम और स्ट्रॉंटियम आधारित डिकारोक्साइलेट्स के संरचनात्मक परिदृश्य की जांच की। तीन aprotic ध्रुवीय सॉल्वेंट्स में दो कठोर और दो लचीला कार्बनिक ligands का उपयोग किया गया था। डीएमएफ, डीएमए, और एमएफ। सभी ठोस पदार्थों की एक महत्वपूर्ण संरचनात्मक विशेषता धातु-कार्बोक्साइल समन्वय से बने कठोर 1 डी स्तंभों की घटना थी। आंतरिक गुणों के अनुसार, सभी छः ठोसों ने विभिन्न तापमान और आवृत्तियों पर दिलचस्प ढांकता हुआ व्यवहार दिखाया। सभी ठोसों ने नीले या नीले-हरे उत्सर्जन के साथ फोटोल्यूमिनेन्स प्रदर्शित किया। अध्याय IIIB में, हमने कार्बोक्साइल समूहों के साथ स्ट्रॉंटियम आयनों के सुपरमोल्यूलर संगठन को तर्कसंगत बनाने के उद्देश्य से पाइरीडिन या एमिनो समूह युक्त तीन अलग कार्बोक्साइलिक एसिड के साथ स्ट्रॉंटियम आयनों के सोलवोथर्मल क्रिस्टलाइजेशन की खोज की है। बहुसंख्यक लिंकर्स (2,5-पीडीसी) और (2-पीजेडसी) के उपयोग से कार्बनिक पुलों द्वारा जुड़े 1 डी स्ट्रॉंटियम कार्बोक्साइल कॉलम द्वारा संचालित 3 डी सीपी का नेतृत्व किया गया। एक लचीला एमिनोडिकारबोक्सिलिक एसिड जैसे आईडीए ने एक और दिलचस्प ठोस नेतृत्व किया, जिसमें एक दुर्लभ असतत एसआरओ 6 एक शीट बनाने वाले कार्बनिक लिंकर के माध्यम से एक दूसरे से जुड़ा हुआ है। चार नए तैयार ठोस पदार्थों की आवृत्ति और तापमान निर्भर ढांकता हुआ व्यवहार की जांच की गई। अध्याय चतुर्थ में, दो वी-आकार वाले लिगेण्डों को विभिन्न समन्वय पॉलिमर तैयार करने के लिए चुना गया था। साहित्य से पता चला है कि, इन दो वी-आकार वाले लिगेण्डों द्वारा बनाए गए अधिकांश एमओएफ / सीपी में संरचना में अतिथि

अणुओं को समायोजित करने के लिए पर्याप्त जगह है। इसलिए, हमारा प्राथमिक उद्देश्य एल्केलाइन-पृथ्वी धातु आधारित एमओएफ / सीपी को अतिथि अणुओं के साथ या उसके बिना तैयार करना था और ठोस पदार्थों के अतिथि निर्भर ढांकता हुआ व्यवहार की जांच करना था। अध्याय वी में, हमने 4,4-सल्फोनील्लिडबेन्ज़िक एसिड के साथ अपना काम बढ़ाया और विभिन्न प्रकार के समन्वय तैयार किए

## TABLE OF CONTENTS

<b>CERTIFICATE.....</b>	<b>i</b>
<b>ACKNOWLEDGEMENTS.....</b>	<b>iii</b>
<b>ABSTRACT.....</b>	<b>v</b>
<b>LIST OF CONTENT.....</b>	<b>xi</b>
<b>LIST OF FIGURES.....</b>	<b>xv</b>
<b>LIST OF TABLES.....</b>	<b>xxvi</b>
<b>LIST OF SCHEMES.....</b>	<b>xxviii</b>
<b>ABBREVIATIONS.....</b>	<b>xxx</b>
<b>Chapter I</b>	
I.1 Introduction.....	1
I.2 Supramolecular chemistry and intermolecular interactions.....	2
I.3 Crystal engineering and supramolecular synthon.....	3
I.4 Porous crystalline materials.....	4
I.5 Coordination polymers CPs or metal-organic frameworks (MOFs): A new class of porous materials.....	6
I.6 Cambridge Structural Database (CSD).....	12
I.7 Coordination polymers CPs or metal-organic frameworks (MOFs) based on <i>s</i> -block metal ions.....	13
I.8 Application of MOFs.....	21
I.9 CPs/MOFs for electronics: Emerging dielectric materials.....	25
I.10 Other application of MOFs materials.....	29

References.....	32
-----------------	----

## **Chapter II**

### **Structural diversity of alkaline-earth 2,5-thiophenedicarboxylates**

II.1 Introduction.....	48
II.2 Alkaline-earth metal and 2, 5-thiophene based chemistry .....	49
II.3 Experimental section.....	56
II.4 Results and discussion.....	61
II.5 Structural landscape of alkaline-earth metal- <i>TDC</i> -solvent.....	74
II.6 Thermal analysis of solids 1-6.....	77
II.7 Photoluminescence properties.....	78
II.8 Conclusion.....	83
References.....	84

## **Chapter IIIA**

### **Ca and Sr based coordination polymers: Synthesis, structure, photoluminescence and dielectric properties.....**

IIIA.1 Introduction.....	89
IIIA.2 Experimental Section.....	91
IIIA.3 Results and discussion.....	96
IIIA.4 Dielectric behaviour of the solids 6-11.....	111
IIIA.5 Photoluminescence properties.....	125
IIIA.6 Thermal analysis of the solids 6-11.....	129
IIIA.7 Conclusion.....	135
References.....	136

## **Chapter IIIB**

### **Strontium and aminodicarboxylate/N-heterocyclic ligand-based coordination polymers: Synthesis, structure and photoluminescence properties**

IIIB.1 Introduction.....	139
IIIB.2 Experimental Section.....	140
IIIB.3 Results and discussion.....	144
IIIB.4 Dielectric properties.....	155
IIIB.5 Structural chemistry of strontium carboxylate.....	162
IIIB.6 Photoluminescence properties.....	163
IIIB.7 Thermal analysis of the solids 12-15.....	166
IIIB.8 Conclusion.....	168
References.....	169

#### **Chapter IV**

#### **Solvent dependent dielectric behavior study of alkaline-earth metals based coordination polymers: Synthesis, structure and photoluminescence properties**

IV.1 Introduction.....	173
IV.2 Cambridge Structural Database (CSD).....	174
IV.3 Experimental section.....	181
IV.4 Results and discussion.....	185
IV.5 Dielectric behavior of all the solids.....	201
IV.6 Thermal analysis.....	213
IV.7 Photoluminescence properties.....	215
IV.8 Conclusion.....	219
References.....	220

## **Chapter V**

### **Manganese(II) sulfonyldibenzoate based coordination polymers: Synthesis, structure, and dielectric properties.....**

V.1 Introduction.....	224
V.2 Cambridge Structural Database (CSD).....	224
V.3 Experimental section.....	233
V.4 Results and discussion.....	238
V.5 Dielectric behavior of the solids 16-21.....	258
V.6 Thermal analysis.....	267
V.7 Conclusion.....	271
References.....	272

## **Chapter VI**

Summary, Conclusions and Future directions.....	273-276
---	---------

### **APPENDIX**

Rietveld refinement of PXRD pattern of solids <b>1-30</b> .....	277-281
ACADEMIC RESUME OF AUTHOR.....	282

## List of Figures

<b>Figure I.1</b> Crystal structure of sodalite (Zeolite).....	6
<b>Figure I.2</b> Venn diagram representing the correlation among metal-organic solids (MOM), coordination polymer (CP), coordination network (CN), and metal-organic framework (MOF) ( <i>Cryst. Growth Des.</i> 2017, 17, 4043–4048).....	8
<b>Figure I.3</b> (a) X-ray single crystal structure of Prussian blue $\text{Fe}_4[\text{Fe}(\text{CN})_6]_3$ ( <i>Cryst. Growth Des.</i> 2017, 17, 4043–4048) (b) A synthetic route and 3D framework structure of MOF-5 showing linkage of BDC ligands with tetranuclear zinc(II) nodes.....	10
<b>Figure I.4</b> Synthetic route and 3D framework structure of HKUST-1 and ZIF-8.....	11
<b>Figure I.5</b> Synthetic route and 3D framework structure of MIL-101 and UiO-66.....	12
<b>Figure I.6</b> Growth of the CSD and MOF entries since 1972 (adapted from <i>Chem. Mater.</i> , 2017, 29, 2618–2625.). The inset shows the formation of MOFs from metal (red) and ligand (blue).....	13
<b>Figure I.7</b> Number of citations containing the keyword “coordination polymers, metal organic framework and alkaline-earth metal coordination polymers” in the past 17 years (source: SciFinder Scholar, 31/12/2017).....	14
<b>Figure I.8</b> Synthesis of $\text{Be}_{12}(\text{OH})_{12}(\text{BTB})_4$ .....	16
<b>Figure I.9</b> Synthesis of $\text{Mg}_2(\text{dobdc})$ (Mg-MOF-74).....	17
<b>Figure I.10</b> Synthesis of 3D framework structure of Ca-SBA and absorption of Xe gas through intermolecular interactions. ....	19
<b>Figure I.11</b> (a) "Antenna effect" observed in Lanthanide based MOFs (b) Various application of luminescent MOFs materials .....	24
<b>Figure I.12</b> Routes for MMOFs preparation: (a) use of short linkers; (b) metalloligand approach; (c) use of radicals as ligands.....	25

<b>Figure I.13</b> Representation of four different polarization mechanism in the dielectric materials.....	26
<b>Figure I.14</b> Dielectric behavior of Sr-based 3D-MOF (adapted from) (a) and ZIF-8 films (b) as well as their MIM device (Inset) (adapted from <i>Chem. Mater.</i> 2015, 25, 27 and <i>J. Mater. Chem. C</i> , 2014, 2, 3762).....	28
<b>Figure II.1</b> Two corner shared polyhedral $\{\text{MgO}_6\}$ bridged by the <i>TDC</i> ligand on the <i>ab</i> -plane.....	63
<b>Figure II.2</b> Magnesium carboxylate extended interaction in <b>1</b> leading to 2D sheets through the dimeric $\{\text{Mg}_2(\text{COO})_4\}$ dimers .....	64
<b>Figure II.3</b> The adjacent 2D sheets are strengthened by C–H···O through uncoordinated carboxylate oxygens.....	64
<b>Figure II.4</b> 2D sheets of solid <b>1</b> on <i>ab</i> -plane. In <b>1</b> , each dimeric unit is connected to four others through <i>TDC</i> . .....	65
<b>Figure II.5</b> Schematic representation of a simple two-dimensional (4,4) <i>sql</i> net in <b>1</b> .....	65
<b>Figure II.6</b> In <b>2</b> , (a) the basic building unit calcium tetramer is formed by the edge-sharing of two octahedra and two pentagonal bipyramids (b) The SBU of the composition, $\text{Ca}_4(\text{COO})_{4/2}(\text{COO})_{4/2} \equiv \{\text{Ca}_4(\text{COO})_4\}$ forms the 2D coordination network. (c) 3D view of the solid <b>2</b> . Solvents molecules omitted for the clarity.....	67
<b>Figure II.7</b> The solid <b>2</b> with <i>pcu</i> topological net.....	68
<b>Figure II.8</b> In <b>3</b> (a) Calcium distorted pentagonal bipyramids share edges chains along [100] and [011] through the SBU $\{\text{Ca}(\text{COO})_{5/5}\}$ . (b) The solvent and water molecules coordinated to the metal atoms are projecting towards the cavities present in the 3D network. ....	69
<b>Figure II.9</b> The solid <b>3</b> with <i>pcu</i> topological net.....	70

<b>Figure II.10</b> In <b>4</b> (a) the dimer $\{\text{Sr}_2(\text{COO})_6\}$ formed by a pair of face shared strontium hendecahedra acts as SBU. (b) The hendecahedra chains are pillared by $\text{TDC}^{2-}$ along [011] plane (c) The solvent molecules coordinated to metal atoms occupy the cavities formed in the 3D rhombic channels. ....	71
<b>Figure II.11</b> The solid <b>4</b> with <i>pcu</i> topological net.....	71
<b>Figure II.12</b> In <b>4</b> , two pentagonal bipyramids share edges to form the dimer i.e $\{\text{Sr}_2\text{O}_{12}\}$ .The dimers are further connected by the ligand forming a strontium-carboxylate network.....	72
<b>Figure II.13</b> In <b>5</b> , (a) The edges shared SBU dimer $\{\text{Sr}_2(\text{COO})_6\}$ extended along [100]. (b) The view of 3D framework on <i>bc</i> -plane, where solvent and water molecules are projected towards the cavities. ....	73
<b>Figure II.14</b> The solid <b>5</b> with <i>pcu</i> topological net.....	73
<b>Figure II.15</b> TG curves for all the solids <b>1-5</b> .....	78
<b>Figure II.15</b> Diffuse reflectance spectra of <b>1-5</b> .....	79
<b>Figure II.17</b> Emission spectra of solids <b>1-5</b> and free <i>TDC</i> ligand.....	79
<b>Figure IIIA.1</b> (a) Edge shared strontium hendecahedra forming zigzag columns. Crystal structure of <b>6</b> viewed along (b) [100] and (c) [010] showing the arrangement of $\{\text{Sr}(\text{COO})_2\}$ units linked through $\text{BDC}^{2-}$ (d) A simplified representation of the column based 3D CP in <b>6</b> . The green columns representing strontium carboxylate units are linked through the ligand <i>BDC</i> (cyan wires).....	100
<b>Figure IIIA.2</b> In solid <b>7</b> , hendecahedra $\{\text{CaO}_8\}$ share triangular faces forming $\{\text{Ca}(\text{COO})_2\}$ column.....	101
<b>Figure IIIA.3</b> (a) Crystal structure of <b>7</b> on <i>bc</i> -plane showing the arrangement of calcium carboxylate columns and organic linkers. (b) The linking of the carboxylate columns and $\text{ABDC}^{2-}$ ligands with disordered amino groups on <i>ab</i> -plane.....	102

<b>Figure IIIA.4</b> A simplified view of the column based 3D CP in <b>7</b> . The strontium carboxylate columns (magenta) are linked through the ligand $ABDC^{2-}$ (cyan wires). .....	102
<b>Figure IIIA.5</b> (a) Edge shared trimers i.e. $\{Ca_3(COO)_6\}$ units. (b) Crystal structure of <b>8</b> on $bc$ -plane showing the arrangement of calcium carboxylate columns and two sets of $ABDC$ ; solvent molecules are omitted for clarity (c) The structure viewed on $ab$ -plane wherein the amino group present on the ligand is ordered (d) The structure viewed on $ac$ -plane wherein the amino group present on the ligand is disordered (e) A simplified view of the column based 3D CP in <b>8</b> . The calcium carboxylate columns (saffron) are linked through $ABDC^{2-}$ (cyan and purple wires denote the ligands with different binding modes).....	104
<b>Figure IIIA.6</b> The $\{Sr(COO)_2\}$ column arises from $SrO_8$ hendecahedra sharing through triangular faces. ....	105
<b>Figure IIIA.7</b> (a) A disordered DMF molecule projected into the vacant channel is shared by two strontium atoms. (b) Crystal structure of <b>9</b> on $bc$ -plane showing the arrangement of strontium carboxylate columns and organic linkers. ....	106
<b>Figure IIIA.8</b> (a) The linking of the carboxylate columns and $ABDC^{2-}$ with disordered amino groups on $ab$ -plane. (b) A simplified view of the column based 3D CP in <b>9</b> . The strontium carboxylate columns (green) are linked through $ABDC^{2-}$ (cyan wires). ....	106
<b>Figure IIIA.9</b> The $\{Sr(COO)_2\}$ column arises from edge shared $SrO_7$ pentagonal bipyramidal polyhedra.....	107
<b>Figure IIIA.10</b> (a) Crystal structure of <b>10</b> on $ab$ -plane showing the arrangement of strontium carboxylate columns and organic linkers. (b) The linking of the carboxylate columns and $OBA^{2-}$ ligands on $bc$ -plane. ....	108
<b>Figure IIIA.11</b> (a) A simplified view of the column based 2D CP in <b>10</b> . The strontium carboxylate columns (green) are linked through the ligand $OBA^{2-}$ (cyan wires). ....	108
<b>Figure IIIA.12</b> (a) Edge shared $SrO_8$ hendecahedron forming zigzag $\{Sr(COO)_2\}$ columns. (b) Crystal structure of <b>11</b> viewed on $ac$ -plane showing the linking of columns through $FBA^{2-}$ along a chain. (c) The structure of <b>11</b> viewed along $c$ -axis. (d) A simplified representation of	

2D CP in **6**. C–H···O and C–H···F interaction with EtOH (pink spheres) further strengthen the sheets. Lattice water (saffron spheres) are involved in hydrogen bonding with EtOH molecules. DMA occurring in the channels interact with coordinated water through H-bonding. ....110

**Figure IIIA.13** Frequency dependent dielectric constant  $\epsilon'$  (a) and (b) dielectric loss ( $\tan \delta$ ) at 293 K. Temperature dependent dielectric constant  $\epsilon'$  (c) and (d) dielectric loss ( $\tan \delta$ ) at 1 KHz.....114

**Figure IIIA.14** Powder X-ray diffraction of solid **11**, as synthesized and after heating at 40, 60, 80, 100, 120 and 140 °C. As observed from the TGA of solid **11**, above 60 °C the compound starts losing solvent molecule this is also in accordance with PXRD pattern which indicates the appearance of new peaks. The solid becomes X-ray amorphous above 140 °C.....115

**Figure IIIA.15-21** Temperature dependent (a) dielectric constant and (b) dielectric loss at constant frequency. Frequency dependent (c) dielectric constant and (d) dielectric loss at various temperatures for **6-11**.....116-122

**Figure IIIA.22** Impedance plots with equivalent circuit of the solids **6-11** and heated sample **11'**.....123

**Figure IIIA.23** (a) Emission ( $\lambda_{ex} = 350$  nm) spectra of the solids **6-11** (b) (i) Optical (Bright field, BF) and (ii) photoluminescence (PL) images ( $\lambda_{ex} = 405$ nm laser) of the solids **6-11**...125

**Figure IIIA.24** (a) Emission ( $\lambda_{ex} = 350$  nm) spectra of ligands (b) (i) Optical (Bright filed, BF) and (ii) photoluminescence (PL) images ( $\lambda_{ex} = 405$ nm laser) of powder sample ligands.....126

**Figure IIIA.25** Photoluminescence emission spectra of ligands at (a)  $\lambda_{ex} = 310$  nm and (b)  $\lambda_{ex} = 405$  nm. (c) Photoluminescence excitation spectra of ligands ( $\lambda_{ex} = 550$  nm).....127

**Figure IIIA.26** Photoluminescence emission spectra of solids **6-11** at (a)  $\lambda_{ex} = 310$  nm and (b)  $\lambda_{ex} = 405$  nm. (c) Photoluminescence excitation spectra of solids **6-11** ( $\lambda_{ex} = 550$  nm)..128

<b>Figure IIIA.27</b> Photoluminescence emission spectra ( $\lambda_{\text{ex}}= 405$ nm diode laser) of (a) ligands and (b) solids <b>1-6</b> . All spectra were recorded by ocean optic Maya Pro spectrometer using 425 nm dichroic mirror.....	128
<b>Figure IIIA.28</b> TG analysis of the solids <b>6-11</b> .....	130
<b>Figure IIIB.1</b> Optical images of the crystals under microscope.....	142
<b>Figure IIIB.2</b> (a) $\{\text{SrO}_6\}$ octahedra bridged by the carboxylate group of $\text{IDA}^{2-}$ ligand forming a chain along [001]. (b) Strontium octahedra bridged to each other through $\text{IDA}^{2-}$ forming a sheet on the <i>ac</i> -plane; hydrogen atoms are omitted for the clarity. (c) Adjacent sheets are linked via C–H···O and N–H···O interactions to form the 3D supramolecular structure. The composition of <b>12</b> is $[\text{Sr}(\text{IDA})_{6/3}] \equiv [\text{Sr}(\text{IDA})_2]$ .....	148
<b>Figure IIIB.3</b> (a) SEM crystal image of <b>12</b> and corresponding (b) mixed EDX maps of individual elements O, Sr, and C, shown separately in (d), (e) and (f) respectively. (c) EDX spectra of <b>12</b> . ....	147
<b>Figure IIIB.4</b> (a) Edge shared strontium dodecahedra $\{\text{SrO}_8\}$ geometry forms a strontium carboxylate column. (b) The strontium polyhedral chains are pillared by the <i>2,5-PDC</i> ligand on <i>ac</i> -plane. (c) A view of 3D rhombic channel framework along [100], where coordinated solvent molecules are projected towards the cavities. Hydrogen atoms are omitted for clarity. The composition of <b>13</b> is $[\text{Sr}(2,5\text{-PDC})_{5/5}(\text{DMF})_{1/1}] \equiv [\text{Sr}(2,5\text{-PDC})(\text{DMF})]$ .....	149
<b>Figure IIIB.5</b> (a) Edge shared strontium dodecahedrons $\{\text{SrO}_8\}$ geometry forms strontium carboxylate columns. (b) The strontium polyhedral chains are pillared by <i>2,5-PDC</i> along [010]. (c) A view of rhombic channel framework on <i>bc</i> -plane where coordinated solvent molecules are projected towards the cavities. Hydrogen atoms are omitted for clarity. The composition of <b>14</b> is $[\text{Sr}(2,5\text{-PDC})_{5/5}(\text{DMA})_{1/1}] \equiv [\text{Sr}(2,5\text{-PDC})(\text{DMA})]$ .....	150
<b>Figure IIIB.6</b> (a) Arrangement of polyhedra chain along the direction of [010]. (b) The arrangement of twelve polyhedra networks on <i>bc</i> -plane. Hydrogens on <i>2-PZC</i> ligands omitted for the clarity.....	151

<b>Figure IIIB.7</b> (a) Arrangement of two twelve polyhedra networks one over the other (b) Arrangements of polyhedron along the direction of [100]. Hydrogen and 2-PZC ligand omitted for the clarity.....	152
<b>Figure IIIB.8</b> Microscopic image of the silver-coated pellets used for the dielectric measurement.....	89
<b>Figure IIIB.9-16</b> Frequency dependent (a) dielectric constant $\epsilon'$ and (b) dielectric loss ( $\tan \delta$ ) at 293 K. Temperature dependent (a) dielectric constant and (b) dielectric loss under the frequency range of 0.1–10 <sup>6</sup> Hz. <b>12-15</b> .....	158-161
<b>Figure IIIB.17</b> Emission spectra (a) ( $\lambda_{\text{ex}} = 350$ nm), (b) ( $\lambda_{\text{ex}} = 360$ nm) of solids <b>12-15</b> . (c) Excitation spectra of solids <b>12-15</b> .....	164
<b>Figure IIIB.18</b> Emission spectra (a) ( $\lambda_{\text{ex}} = 350$ nm) and (b) ( $\lambda_{\text{ex}} = 360$ nm) of the free ligands. (c) Excitation spectra of the free ligands.....	165
<b>Figure IIIB.19</b> TG analysis of the solids <b>12-15</b> .....	166
<b>Figure IV.1</b> A number of structures reported in the literature with different metals and two V-shaped ligands. ....	174
<b>Figure IV.2</b> (a) Trimeric {Mg <sub>3</sub> O <sub>16</sub> } SBU unit containing three corners shared octahedral polyhedrons. (b) Trimeric {Mg <sub>3</sub> O <sub>16</sub> } SBU chains bridged by the <i>FBA</i> <sup>2-</sup> chain resulting in a 2D sheet structure on <i>bc</i> -plane. Hydrogen atoms and DMF molecules omitted for the clarity. ....	188
<b>Figure IV.3</b> Crystal structure of <b>16</b> viewed on <i>ac</i> -plane showing the linking of trimeric {Mg <sub>3</sub> O <sub>16</sub> } SBU unit through <i>FBA</i> <sup>2-</sup> ligands resulting in a 1D square shaped channel. The coordinated water molecules are involved in O–H···O interaction with the DMA solvent molecules. DMA molecules reside in the square shaped channel form by the structure (See inset). Hydrogen atoms on benzene ring omitted for the clarity. ....	189
<b>Figure IV.4</b> Two 1D square shaped chains supported by the C–H···F intermolecular interaction to form the 3D structure on <i>ac</i> -plan. Fluorine atoms on the <i>FBA</i> <sup>2-</sup> ligand are	

involved in C–H···F interaction with the DMF solvent molecules coordinated to calcium atom. Hydrogen atoms on benzene ring omitted for the clarity.....189

**Figure IV.5** 1D chain of face shared dodecahedron polyhedrons  $\{\text{CaO}_8\}_n$  bridged by the carboxylate groups of  $\text{FBA}^{2-}$  ligand along [001].....191

**Figure IV.6** (a) 2D representation of **17**. The 1D chains are bridged by the  $\text{FBA}^{2-}$  ligand to form the 2D network on the *ac*-plane. (b) View of 3D rhombic channel structure along the [001] direction. Coordinated solvents DMF reside in the channels. Hydrogen atoms omitted for the clarity.....191

**Figure IV.7** Tetramer,  $\{\text{Ca}_4\text{O}_{22}\}$  made of three pentagonal bipyramidal and one distorted dodecahedron forming a continuous metal-carboxylate column.....193

**Figure IV.8** (a) 2D representation of solid **18** where tetramer chains are bridged by the  $\text{SBA}^{2-}$  ligand on *ac*-plane. (b) 3D structure showing the metal coordinated DMF solvent molecules are involved in C–H···O interaction with lattice DMF.....193

**Figure IV.9** (a) 1D chain of edge-shared pentagonal bipyramidal polyhedrons (b) Pentagonal bipyramidal  $\{\text{SrO}_7\}$  polyhedrons bridged by the carboxylate group of  $\text{SBA}^{2-}$  ligand forming a 2D network on *bc*-plane .....195

**Figure IV.10** Crystal structure of **19** on *ac*-plane showing the linkage of  $\text{FBA}^{2-}$  ligand to the metal ions forming a square-shaped continuous chain. The coordinated water molecules are involved in O–H···O interaction with the DMA solvent molecules. DMA molecules reside in the channel form by the structure (See inset). Hydrogen atoms and DMA molecules omitted for the clarity. ....195

**Figure IV.11** 2D structure of **19** on *ab*-plan, Metal-carboxylate chain is bridged by the  $\text{FBA}^{2-}$  ligands.....196

**Figure IV.12** The two metal-carboxylate chains are supported by the C–H···F intermolecular interaction to form the 3D structure on *ac*-plan. Fluorine atoms on the  $\text{FBA}^{2-}$  ligand are involved in C–H···F interaction with the DMF solvent molecules coordinated to calcium atom. Hydrogen atoms on benzene ring omitted for the clarity. ....196

<b>Figure IV.13</b> Pentagonal bipyramidal geometry {SrO <sub>7</sub> } polyhedrons bridged by the carboxylate group of SBA <sup>2-</sup> ligand forming a chain along [001].....	198
<b>Figure IV.14</b> (a) Ladder type network of <b>20</b> viewed along the <i>b</i> -axis. (b) Pentagonal bipyramidal polyhedrons {SrO <sub>7</sub> } bridged by the carboxylate group of SBA <sup>2-</sup> ligand forming a 2D network on <i>bc</i> -plane.....	198
<b>Figure IV.15</b> 3D supramolecular network of <b>19</b> viewed along the <i>b</i> -axis. The two ladder types of arrangements are supramolecularly supported by the two different intermolecular interactions (O–H···O, blue dotted line, and C–H···O pink dotted line).....	199
<b>Figure IV.16</b> Face shared distorted dodecahedron {BaO <sub>8</sub> } polyhedrons bridged by the carboxylate group of FBA <sup>2-</sup> ligand forming a 1D chain along [001].....	200
<b>Figure IV.17</b> (a) 2D representation of <b>21</b> . The 1D chains are bridged by the FBA <sup>2-</sup> ligand to form the 2D network on the <i>ac</i> -plane. (b) View of the 3D rhombic channel structure of <b>21</b> along the direction [001]. Coordinated solvents DMA reside in the channels. Hydrogen atoms omitted for the clarity.....	201
<b>Figure IV.18-27</b> Frequency dependent (a) dielectric constant and (b) dielectric loss at various temperatures for <b>16-21</b> and heated samples. Temperature dependent (c) dielectric constant and (d) dielectric loss under the frequency range of 0.1–10 <sup>6</sup> Hz.....	207-212
<b>Figure IV.28</b> TG curve of the solids <b>16-21</b> .....	254
<b>Figure IV.29</b> Emission spectra of (a) the free ligands and (b) the solids <b>16-21</b> .....	215
<b>Figure IV.30</b> Powder X-ray diffraction patterns of solids (a) <b>16</b> and (b) <b>18</b> at different temperatures.....	216
<b>Figure IV.31</b> Powder X-ray diffraction patterns of solids (a) <b>19</b> and (b) <b>20</b> at different temperatures.....	216

<b>Figure V.1</b> (a) Number of solids reported in the literature based on <i>SBA</i> ligands and different metal ions. (b) Percentage of different SBU present in the Mn- <i>SBA</i> system reported in the literature. . . . .	226
<b>Figure V.2</b> (a) Pentanuclear clusters $\{\text{Mn}_5\text{N}_2\text{O}_{24}\}$ in <b>22</b> . (b) $\text{Mn}_5$ clusters connected to each other by four <i>SBA</i> <sup>2-</sup> forming a 2D sheet. Hydrogen atoms omitted for the clarity. . . . .	244
<b>Figure V.3</b> A view of 1D chain along [101] showing the bridging of pentanuclear $\{\text{Mn}_5\text{N}_2\text{O}_{24}\}$ clusters by <i>SBA</i> <sup>2-</sup> . . . . .	244
<b>Figure V.4</b> In <b>22</b> , two 1D chains are further stabilized by the coordinated (blue) and the lattice (magenta) solvent (DMA) through C–H···O. While the coordinated DMA interacts with the carboxylate oxygen of <i>SBA</i> <sup>2-</sup> , the lattice DMA interacts with benzene moiety. . . . .	245
<b>Figure V.5</b> (a) A view of trimeric unit present in <b>23</b> (b) 2D sheets in <b>23</b> ; trimeric clusters bridged by <i>SBA</i> <sup>2-</sup> forms chains which are also linked to each other through the ligand. . . . .	246
<b>Figure V.6</b> The sheets on <i>ab</i> plane interact through C–H···O between sulfonyl oxygen and benzyl hydrogen. . . . .	247
<b>Figure V.7</b> (a) View of two different SBU i.e. tetramer $\{\text{Mn}_4\text{O}_{20}\text{N}_2\}$ and dimer $\{\text{Mn}_2\text{O}_8\text{N}_2\}$ in the structure (b) 2D representation of <b>25</b> , chains made of tetramer cluster bridged by the <i>SBA</i> <sup>2-</sup> on the <i>bc</i> -plane. Hydrogen atoms omitted for the clarity. . . . .	249
<b>Figure V.8</b> 3D view of <b>25</b> viewed along the [001] direction. $\text{H}_2\text{O}$ molecules bonded to DMA solvent molecules through C–H···O interaction reside in the channels. Hydrogen atoms on <i>SBA</i> and <i>pyz</i> omitted for the clarity. . . . .	250
<b>Figure V.9</b> (a) $\{\text{Mn}_2\text{O}_7\text{N}_4\}$ dimer made of distorted octahedral and square pyramidal units bridged by two <i>SBA</i> ligands. (b) 2D sheets in <b>27</b> wherein dimers are bridged by <i>SBA</i> <sup>2-</sup> . . . . .	251

<b>Figure V.10</b> In <b>27</b> , the sheets on <i>bc</i> plane are further stabilized by two type of solvents. One type of DMA ( <b>magenta</b> ) interact through C–H···O <sub>w</sub> (O <sub>w</sub> - coordinated water) while the lattice DMA ( <b>blue</b> ) link the chains via C–H···O <sub>S</sub> (O <sub>S</sub> – sulfonyl oxygen).....	252
<b>Figure V.11</b> The solid <b>27</b> viewed along [010].The lattice DMA interacts with both sulfonyl O and H of <i>phen</i> through C–H···O.....	253
<b>Figure V.12</b> (a) A view of the trimeric {Mn <sub>3</sub> N <sub>2</sub> O <sub>14</sub> }cluster.(b) {Mn <sub>3</sub> } clusters bridged by SBA <sup>2-</sup> forming a 2D sheet. Hydrogen atoms are omitted for clarity.....	254
<b>Figure V.13</b> Crystal structure of <b>28</b> viewed along [100].....	255
<b>Figure V.14</b> (a) A view of the trimeric cluster in <b>29</b> . (b) 1D chain of the trimeric units bridged by SBA <sup>2-</sup> along [001].....	256
<b>Figure V.15</b> Notice how the two non-extendable ligands, <i>phen</i> and <i>acetate</i> facilitate the growth through C–H···O <sub>acetate</sub> ( <b>magenta</b> ) and C–H···O <sub>SBA<sup>2-</sup></sub> ( <b>violet</b> ).....	257
<b>Figure V.16</b> 1D chains in <b>29</b> built of trimeric clusters bridged by SBA <sup>2-</sup> .....	257
<b>Figure V.17</b> 2D H-bonded supramolecular layers in <b>29</b> .....	258
<b>Figure V.18-26</b> Frequency dependent (a) dielectric constant and (b) dielectric loss at various temperatures for <b>22-30</b> .Temperature dependent (a) dielectric constant and (b) dielectric loss under the frequency range of 0.1–10 <sup>6</sup> Hz.....	262-266
<b>Figure V.27</b> TG curve of solids <b>22-30</b> .....	268

## List of Tables

<b>Table I.1</b> Some of the well-known MOFs with their surface area and gas storage capacity are reported in .....	22
<b>Table I.2</b> Selected examples of MOFs-catalyzed reactions .....	23
<b>Table I.3</b> Low- $\kappa$ MOFs ( $f=0.1$ MHz) reported in the literature. ....	29
<b>Table II.1</b> Structural diversity of the compounds crystallized from the system Alkaline earth metal-TDC-solvent reported here as well as literature.....	50
<b>Table II.2</b> Crystal data and structural refinements for <b>1–5</b> .....	60
<b>Table II.3</b> Alkaline-earth-TDC-Solvent system.....	74
<b>Table II.4</b> Summarise the weight loss of solvent molecules in each case .....	77
<b>Table II.4</b> List of bond length ( $\text{\AA}$ ) and bond angles ( $^\circ$ ) of solids <b>1-5</b> .....	80
<b>Table IIIA.1</b> Solids reported in this work as well as literature with the ligands in different solvents used in this study.....	90
<b>Table IIIA.2</b> Crystal data and structural refinements for solids <b>6, 8, 10</b> and <b>11</b> .....	95
<b>Table IIIA.3</b> A comparison of the crystal data of <b>7</b> and <b>9</b> with reported structures.....	98
<b>Table IIIA.4</b> Thermal stability and ( $\epsilon'$ ) measurement temperature range .....	111
<b>Table IIIA.5</b> Dielectric constant of alkaline-earth metal coordination polymers at higher and lower frequency reported in the present work as well as literature.....	112
<b>Table IIIA.6</b> Related parameters derived from impedance plots for solids <b>6-11</b> and <b>11'</b> ...	124
<b>Table IIIA.7</b> Selected bond lengths ( $\text{\AA}$ ) and bond angles ( $^\circ$ ) of solids <b>6-11</b> .....	131
<b>Table IIIB.1</b> Crystal data and structural refinements for solids <b>12-15</b> .....	143
<b>Table IIIB.2</b> Solids where in strontium occurs in an octahedral geometry .....	148

<b>Table IIIB.3</b> A comparison of bond distances ( $\text{\AA}$ ) between coordinated amine groups, coordination numbers and dimensionality in nitrogen-containing ligands .....	153
<b>Table IIIB.4</b> Selected bond lengths ( $\text{\AA}$ ) and angles ( $^\circ$ ) for solids <b>12-15</b> .....	167
<b>Table IV.1</b> Summary of CPs prepared from group (II) metals and 4,4-sulphonyldibenzoic acid ( <i>SBA</i> ).....	175
<b>Table IV.2</b> Crystal data and structural refinements for solids <b>16-21</b> .....	184
<b>Table IV.3</b> (a) Thermal stability and ( $\epsilon'$ ) measurement temperature range for the solid <b>16-21</b> . (b) Solids heated at different temperature and ( $\epsilon'$ ) measurement temperature range ....	205
<b>Table IV.4</b> Dielectric constant of alkaline-earth metal coordination polymers at higher and lower frequency reported in the present work.....	213
<b>Table IV.5</b> Selected bond lengths ( $\text{\AA}$ ) and bond angles ( $^\circ$ ) of solids <b>16-21</b> .....	216
<b>Table V.1</b> Structural diversity of manganese- <i>SBA</i> -auxiliary ligand system reported in the literature. The table also shows the solids prepared in this study for comparison.....	227
<b>Table V.2</b> Crystal data and structure refinement details for <b>22-30</b> .....	237
<b>Table V.3</b> Dielectric constant of solids <b>22-30</b> at higher and lower frequency reported in the present work.....	267
<b>Table V.4</b> Selected bond lengths ( $\text{\AA}$ ) and angles ( $^\circ$ ) for solids <b>22-30</b> .....	269

## List of Scheme

<b>Scheme I.1</b> Relationship between molecular (typically an organic compound) and supramolecular synthesis.....	2
<b>Scheme I.2</b> Common homo and heterosynthons found in acid, amide, and pyridine based functional groups.....	4
<b>Scheme I.3</b> Classification of porous materials based on their pore size.....	5
<b>Scheme I.4</b> Transition from molecular to extended coordination solid. In a coordination complex, the coordination bond is restricted to only a molecule (0D). Intermolecular interactions are essentially through noncovalent bond. In a CP, extended coordination interactions occur in one- or two- or three-dimensions. MOF is a special case of a 3D CP....	7
<b>Scheme I.5</b> Different techniques employed for crystallization of multicomponent solids.....	9
<b>Scheme II.1</b> Synthetic protocol for the crystallisation of solids in the systems $M^{2+}$ -TDC-solvent (M = Mg, Ca or Sr and solvent = DMF, DMA or DEF).....	59
<b>Scheme II.2</b> Linkage of the carboxylate groups of the ligand with metal ions in the solids present in (a) <b>1</b> , (b) and (c) <b>2</b> , (d) <b>3</b> , (e) <b>4</b> and (f) <b>5</b> .....	61
<b>Scheme II.3</b> Coordination environment of the metal atom and its polyhedron in the solids (a) <b>1</b> , (b) and (c) <b>2</b> , (d) <b>3</b> , (e) <b>4</b> and (f) <b>5</b> .....	62
<b>Scheme IIIA.1</b> Synthetic protocol for the crystallization of the solids <b>6-11</b> (M = Ca or Sr and solvent = DMF, DMA or MF).....	91
<b>Scheme IIIA.2</b> Linkage of the carboxylate groups of the ligand with metal ions in the solids present in (a) <b>6</b> , (b) <b>7</b> , (c) and (d) <b>8</b> , (e) <b>9</b> , (f) and (g) <b>10</b> , and (h) <b>11</b> .....	96
<b>Scheme IIIA.3</b> Coordination environment of the metal atom and its polyhedron in the solids (a) <b>6</b> , (b) <b>7</b> , (c) and (d) <b>8</b> , (e) <b>9</b> , (f) <b>10</b> , and (g) <b>11</b> .....	97

<b>Scheme IIIB.1</b> Synthetic protocol for the crystallization of solids <b>12-15</b> (M = Sr and solvent = DMF and DMA).....	144
<b>Scheme IIIB.2</b> Linkage of the carboxylate groups and nitrogen atom of the ligand with metal ions in the solids present in (a) <b>12</b> , (b) <b>13</b> , (c) <b>14</b> , (d) and (e) <b>15</b> .....	145
<b>Scheme IIIB.3</b> The coordination environment of the metal atom and its polyhedron in the solids (a) <b>12</b> , (b) <b>13</b> , (c) <b>14</b> , (d) and (e) <b>15</b> .....	145
<b>Scheme IV.1</b> Synthetic route for the formation of solids <b>16-21</b> from metal salts and ligands.....	185
<b>Scheme IV.2</b> Linkage of the carboxylate groups of two different ligands with metal ions in the solids present in (a) <b>16</b> , (b) <b>17</b> , (c), (d) and (e) <b>18</b> , (f) <b>19</b> , (g) <b>20</b> and (h) <b>21</b> .....	185
<b>Scheme IV.3</b> Coordination environment of the metal atom and its polyhedron in the solids (a) and (b) <b>16</b> , (c) <b>17</b> , (d), (e), (f) and (g) <b>18</b> , (h) <b>19</b> , (i) <b>20</b> and (j) <b>21</b> .....	186
<b>Scheme V.1</b> Synthetic protocol employed for the crystalization of the solids <b>22-30</b> .....	239
<b>Scheme V.2</b> Coordination modes of $SBA^{2-}$ with Mn(II) in the solids <b>22-30</b> .....	240
<b>Scheme V.3</b> Coordination environment of Mn(II) in the solids <b>22-30</b> .....	242

## Abbreviations

1. *TDC* = 2, 5-thiophenedicarboxylic acid
2. *DMF* = N, N'-dimethyl formamide
3. *DEF* = N, N'-diethyl formamide
4. *MF* = N-methylformamide
5. *DMA* = N, N'-dimethyl acetamide
6. *EG* = ethylene glycol
7. *BDC* = 1, 4-benzenedicarboxylic acid
8. *ABDC* = 2-aminoterephthalic acid
9. *OBA* = 4,4'-oxybis(benzoic acid)
10. *FBA* = 4,4'-(hexafluoroisopropylidene)bis(benzoic acid)
11. *IDA* = iminodiacetate
12. *2,5-PDC* = 2,5-pyridinedicarboxylate
13. *2-PZC* = 2-pyrazinecarboxylate
14. *SBA* = 4,4'-sulfonyldibenzoic
15. *2-pic* = 2-picolinic acid
16. *pyz* = 2-pyrazinecarboxylic acid
17. *mpyz* = 5-methyl-2-pyrazinecarboxylic acid
18. *phen* = 1,10-phenanthroline
19. *Ace* = acetate ion